Pergamon

Journal of Structural Geology, Vol. 16, No. 6, pp. 753 to 767, 1994

0191-8141/94 $07.00+0.00

Bedding parallel veins and their relationship to folding

M. W. JESSELL, C. E. WILLMAN* and D. R. GRAY

Victorian Institute of Earth and Planetary Sciences, Department of Earth Sciences, Monash University, Melbourne, Victoria 3168, Australia

(*Received* 3 *April* 1992; *accepted in revised form* 18 *July* 1993)

Abstract—Laminated bedding parallel veins hosted in turbiditic sandstone shale sequences from central Victoria, Australia, consist of stacked, millimetre thick, sub-parallel sheets of quartz separated by micaceous layers, wall rock slivers and pressure solution seams. They have very high length to thickness ratios, are laterally continuous over tens to hundreds of metres, and have relatively uniform thickness compared to other vein types. They are intimately associated with and folded by chevron folds, and the quartz grain shape elongation lineation is commonly orthogonal to mesoscopic and macroscopic fold hinge lines. The bedding parallel veins have two morphological forms. Type I are thin (commonly 5–10 cm) laminated veins which have complex microstructures dominated by phyllosilicate inclusion surfaces, related to oblique opening along bedding with varying rates of deposition (opening) relative to shear displacement (slip) along the bedding surfaces. More common are Type II, thicker (generally <20 cm), banded veins of alternating milky-white quartz with wall rock inclusion laminae (formerly fragments) bounded by stylolitic partings parallel to both bedding and the vein margins. The inclusion surfaces in Type I veins track the opening direction during vein formation. Vein opening-sense criteria suggest cyclical pore fluid pressure fluctuations which predate the amplification and propagation of the host chevron folds; i.e. prior to attainment of significant limb dip. Different layer parallel shortening and amplification rates for individual layers within the sedimentary sequence may lead to bedding parallel veins with an opening sense unrelated to the flexural slip folds which eventually follow.

INTRODUCTION

INTERLAYER slip is considered an important part of flexural folding in low grade metamorphic rocks where movement on bedding surfaces is recorded by slickensides and shear veins (Ramsay 1974, Behzadi & Dubey 1980, Tanner 1989). Shear veins range from stepped, overlapping fibre sheets (e.g. Ramsay & Huber 1983, fig. 13.36, Tanner 1989, 1990) to bedding parallel veins which have more uniform thickness and lateral continuity over tens of metres (e.g. Nicholson 1964, 1978, Fitches *et al.* 1986, Tanner 1989). Bedding parallel veins are a type of vein formed between bedding surfaces where the differential movement is often considered to be sub-parallel to bedding. Bedding parallel veins are common in chevron-folded sequences and have been attributed to flexural slip during folding (e.g. Tanner 1989), post-diagenesis, fluid over-pressuring of detachments in sediments buried to depths of several hundred metres prior to cleavage development and folding (Fitches *et al.* 1986), hydraulic pumping either during folding (Cosgrove 1993) or as post-cleavage 'water sills' or syn-tectonic veins (Mawer 1987, Henderson *et al.* 1990). A complex vein microstructure composed of phyllosilicate inclusion bands, elongate columnar quartz grains and wall rock inclusion fragments, overprinted by patchy dynamic recrystallization and tectonic stylolites, is commonly found.

Chevron folds occur in regularly bedded rocks (de Sitter 1964, Ramsay 1974, Tanner 1989). Slip along layer interfaces is necessary for this folding mechanism (Ramsay 1967, pp. 440–449, 1974), but the position and amount of slip varies both spatially and temporarily and need not take place between all layers (Ghosh 1968, Behzadi & Dubey 1980, Tanner 1989). The positions of bedding parallel veins have been used to relate bedding slip increments to the overall development of chevron folds (Tanner 1989).

This paper examines bedding parallel veins from a chevron-folded quartz-rich turbidite succession in south eastern Australia (Fig. 1). Observations are based on detailed structural mapping and sampling at three localities where veins are continuously exposed around mesoscopic parasitic fold closures (Central Deborah Mine, Bendigo; Little Bendigo, Castlemaine; White Hills, Campbells Creek, south of Castlemaine), as well as vein samples from the limbs of major regional folds at Bendigo (eastern limbs of the Napoleon and Garden Gulley anticlines, Fig. 1 and Appendix Table A1). Information on spacings of veins, lateral continuity of veins and the nature of their host lithologies has been obtained from old 1:360 scale mine plans from 10 mines in the historic Bendigo goldfield (Fig. 1 and Appendix Table A2). Recent geological mapping by Clive Willman at 1:10,000 scale in the Bendigo (Spring Gulley, Golden Square and Eaglehawk Map sheets: Willman & Wilkinson 1992) and Castlemaine areas (Willman in preparation) has shown that the exposures studied are probably the only remaining localities where bedding parallel veins are observed continuously across fold hinges. Deep weathering combined with urban land development in the Bendigo and Castlemaine areas severely limits exposure.

In this paper geometrical relationships of these veins to host folds, as well as meso- and microstructural

*Current address: Victorian Geological Survey, Bendigo, Victoria 3550, Australia.

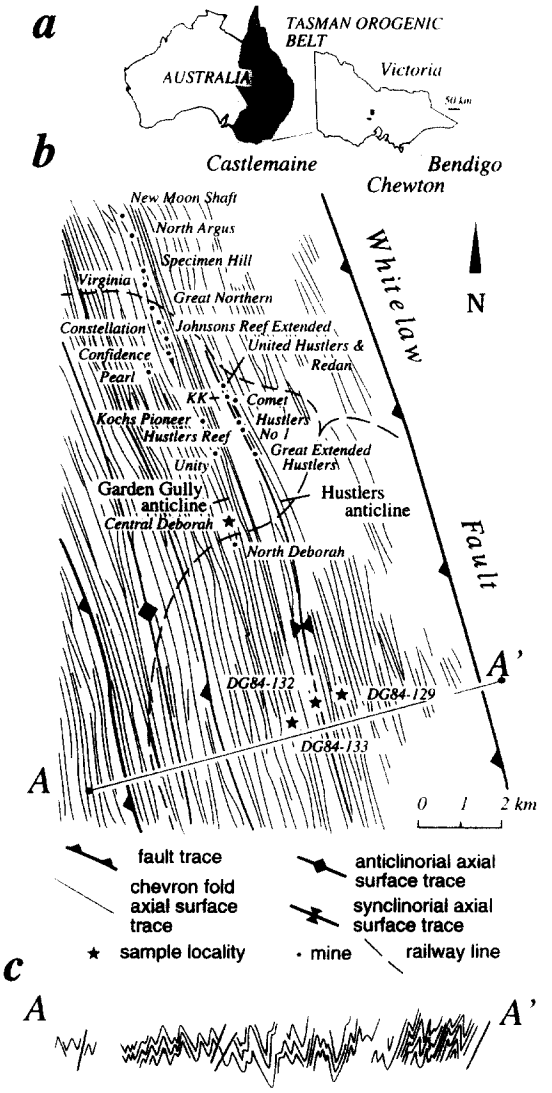

Fig. 1. Geological and structural maps of the historic Bendigo goldfield, Australia. (a) Location map showing position of terrain with respect to the Tasman Orogenic Belt. (b) Fold axial surface trace map showing locations of the mines where bedding parallel vein data were collected (see Table 1). For reference the location of the Comet Mine is 144°17'E 36°45'S, and the Little Bendigo area is south of the main map near Castlemaine (144°14'E 37°4'S). (c) Structural profile of the Bendigo goldfield showing the close to tight chevron style of folding (only major folds shown, modified from Gray & Williams 1991b, fig. 6a).

aspects of the veins are used to show that, during fold initiation and the early stages of folding, slip is characterized by quasi-cyclical hydraulically-controlled opening increments. These episodic bedding parallel dilations may control the nucleation sites of folds and establish buckling instabilities in a layered rock sequence in the early stages of the folding process. The microstructures in these bedding parallel veins suggest that fluid pressure fluctuations must play an important part in the early development of natural chevron folds. Folds may develop in a stick-slip fashion with bedding plane slip (Cosgrove 1993). The work here suggests that for the folds in the Bendigo region this behaviour predominates in the pre-amplification–propagation stages of folding.

SETTING OF THE BEDDING PARALLEL VEINS

The bedding parallel veins occur in a chevron-folded quartz-rich turbidite succession which is part of an E-directed, imbricate-fan thrust system in the Bendigo–Ballarat zone of the Palaeozoic Lachlan Fold belt, eastern Australia (Cox *et al.* 1991, Gray & Willman 1991a,b, Gray *et al.* 1991a). The Bendigo–Ballarat zone surface geology is dominated by major W-dipping, meridional strike-parallel reverse faults which truncate meridional regional anticlinoria and synclinoria (Gray *et al.* 1988, Gray & Willman 1991a,b). These faults are 50–100 km long with throws upwards of 1 km and generally place lowermost Ordovician (Lancefieldian) over uppermost Lower Ordovician (Darriwilian–Yapeenian) rocks. Within individual thrust sheets there is a general westward younging in stratigraphy and a gentle westerly dip of the regional fold enveloping surface. Rocks in the zone consist of an original 4 km thick sequence of Lower to Upper Ordovician quartz rich turbidites overlying Cambrian volcanic rocks and volcanoclastic sedimentary rocks.

Regional folds have wavelengths of 10–15 km and amplitudes in the order of 1–2 km. Parasitic folds define several orders of folding with lower order fold wavelengths ranging from 40 to 300 m and amplitudes from 15 to 100 m. Chevron folds occur in extremely regular fold trains reflecting some 50–65% shortening within thrust-sheets. In the Bendigo region and Chewton–Castlemaine areas where bedding parallel veins are relatively common, major fold axial surface traces are spaced at approximately eight per km (Fig. 1). The folds show slaty cleavage developed in mudstones and a stripy differentiated layering in some sandstones (cf. Stephens *et al.* 1979, Waldron & Sandiford 1988). Hinges within sandstone-dominant facies are more rounded, whereas those in mudstone-dominant sections are more angular. Limb-thrusts and saddle reefs associated with the bedding parallel veins are relatively common. Quartz vein networks are associated with reverse faults, saddle reefs, subhorizontal spurs and tension gashes (Chace 1949, Gray *et al.* 1991b).

Marked gradients in strain occur between the upper and lower parts of individual thrust sheets (Gray & Willman 1991b). Upper parts of thrust sheets have upright, close chevron folds (interlimb angles: 35–50°) with fold axes subparallel to major fault traces, spaced cleavage and both E- and W-dipping reverse faults. They show low strains (X:Z strains $< 5:1$) and subvertical extensions shown by straight quartz-fibres in pressure-shadows on framboidal pyrite in mudstone. Lower parts of thrust sheets are characterized by tight inclined chevron folds (interlimb angles $< 30°$) with predominantly W-dipping axial surfaces, high strains (X:Z $> 30:1$), intense phyllitic cleavage with a strong down-dip mineral stretching lineation, and long curved tapering quartz pressure-shadows on pyrite in mudstone.

Such differences in fold geometry, the intensity of the cleavage and the geometry of quartz-fibres in pressure-

shadows, has been related to internal deformation of thrust sheets during the initiation and propagation of subsurface detachment faults and to their emplacement to shallower crustal levels (Gray & Willman 1991b).

ASSOCIATIONS OF THE BEDDING PARALLEL VEINS

Surface mapping has not established the distribution or frequency of bedding parallel vein occurrences, but old mine plans provide evidence that they are not uniformly distributed. Mine cross-sections from Bendigo show a very high bedding parallel vein frequency which amounts to one for every 10–15 m (stratigraphic thickness) along the Hustlers Line (Whitelaw 1914) and along the Garden Gully Line in the Confidence Mine (Whitelaw 1918) (Fig. 1). This high frequency is reflected by the abundance of saddle reefs.

Regionally, an unequal lateral distribution of bedding parallel veins may correlate with the siting of gold belts. Also, the distribution of bedding parallel veins vertically may be biased towards certain stratigraphic horizons. This may explain the broad stratigraphic control that concentrates mineralization in Lancefieldian, Bendigonian and Chewtonian rocks. Early workers noted this association and termed it the 'favourable bed' theory (Thomas 1953).

Bedding parallel veins have remarkable continuity and have been traced in mine workings for over 3.2 km along strike (Victory Back; Whitelaw 1918) and up to 365 m down-dip (Kochs Pioneer Mine; Stilwell 1917) (Fig. 1). A large number of accurate 1:360 mine plans from Victorian Mines Department document that bedding parallel veins almost always occur on both limbs of individual folds at a given stratigraphic level. This was common knowledge amongst miners during the late 19th and early 20th centuries and was used as a guide for mine development to locate either the rich saddle reef at the apex of a fold or the opposite bedding parallel vein. Mine sections (e.g. Fig. 2a) show that bedding parallel veins are fairly continuous down dip. Mine development only rarely traced bedding parallel veins continuously from one fold hinge to another due to the focus of mining at anticlinal hinges. However Dunn (1896) illustrates a vein in the Johnsons Reef Extended Mine which was traced over the anticline at the 433′ level and then under the syncline at the 521′ level, a total down-dip distance of 85 m (Fig. 2b). The vein is parasitically folded near the fold hinge. Parasitic folding at an anticlinal hinge was also recorded by Whitelaw (1914) from the No. 43 reef of the Hustlers Reef Mine. Bedding parallel veins which

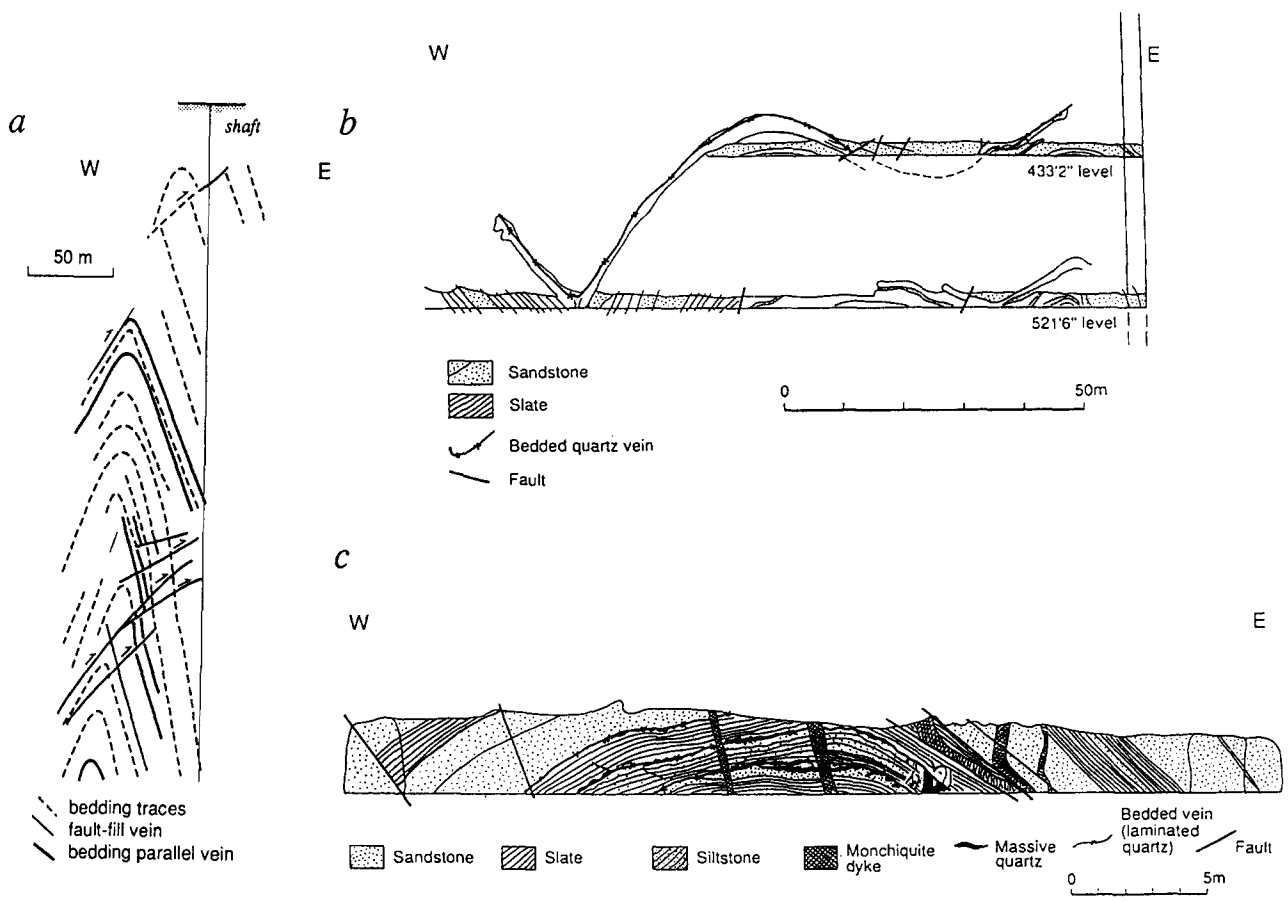

Fig. 2. Associations of bedding parallel veins. (a) Mine section Deborah Anticline, North Deborah Mine, Bendigo, based on 1:360 scale mine plans showing details of the distribution and structure of bedding parallel veins (modified after Caldwell 1942, Cox *et al.* 1991b). (b) Geological section of the Johnsons Reef Extended Mine, Bendigo, showing a bedding parallel vein extending for over 85 m (modified from Dunn 1986). (c) Structural profile of the No. 2 West cross-cut, No. 2 level, Central Deborah Mine, Bendigo, showing folded bedding parallel veins cut by monchiquite dykes.

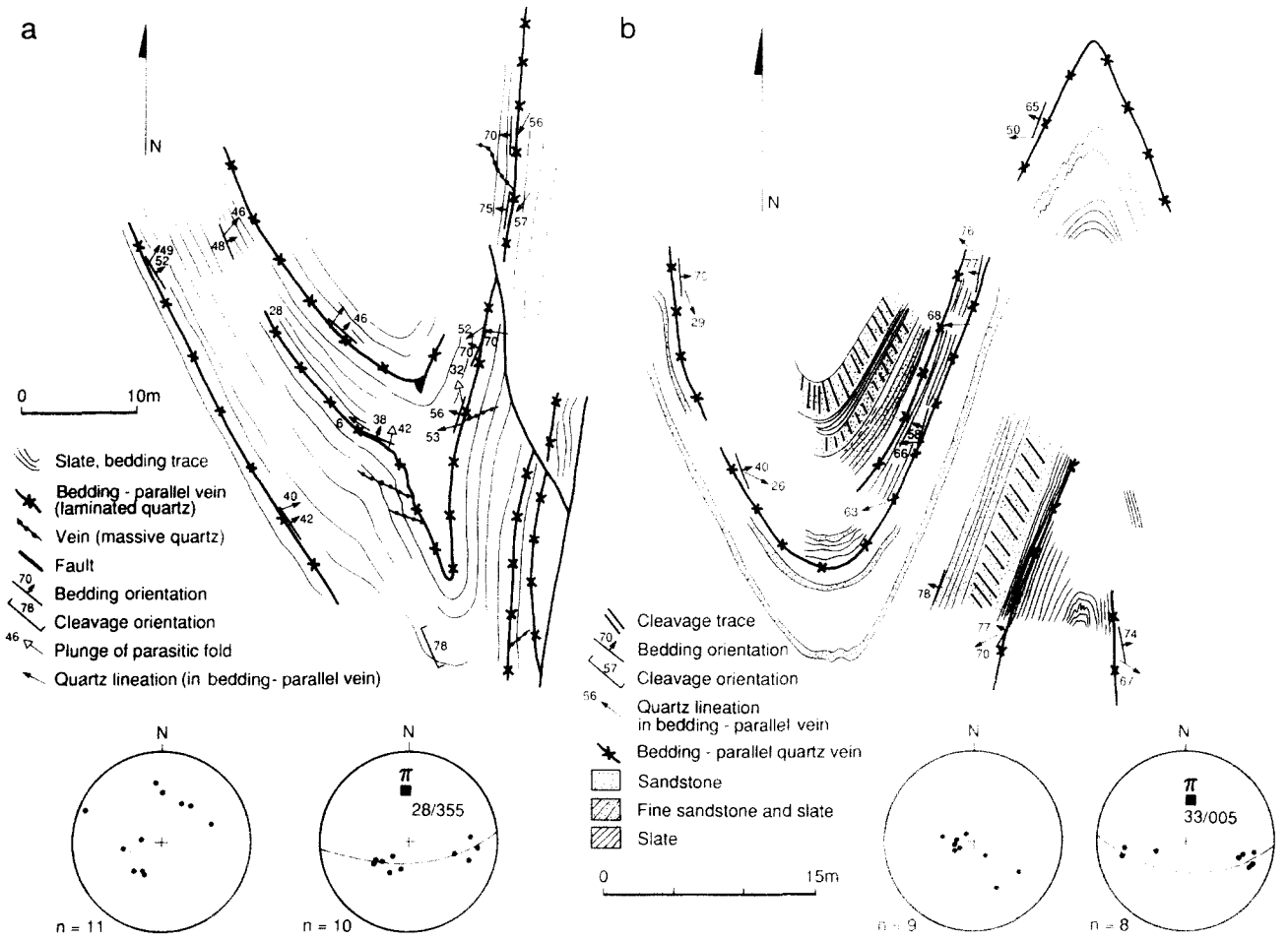

Fig. 3. Geological maps of bedding parallel vein outcrops. (a) Little Bendigo, Castlemaine region (144°14'E 37°4'S). (b) White Hills, Campbells Creek (south of Castlemaine). Equal-area lower-hemisphere projections for each map show the folded quartz-fibre lineation pattern from the mapped bedding parallel vein (left) and girdles of poles to bedding with the determined π axes (right).

close across minor folds are always folded in the hinge zones (Figs. 2c, 3 and 4). Many are cut and displaced by a strong axial plane solution cleavage. Although bedding parallel veins were relatively common in the underground workings of Bendigo, present day field exposures of complete bedding parallel veins are rare. Consequently, detailed observations have been limited to two outcrops (Fig. 3). At Little Bendigo, near Castlemaine, a bedding parallel vein is exposed around the hinge of a syncline which shows hinge collapse, splay veins and 'pseudo-breccia' (Fig. 3a). The main vein varies in width from 0.1 to 15 cm and is continuous around the synclinal hinge for approximately 70 m (Fig. 6). It has three splay veins which branch off the main bedding parallel vein at irregular intervals either from top or bottom of the vein (Fig. 6a). The vein is thickest at the hinge, decreasing in thickness down the limbs, although there is considerable variation in thickness (Fig. 6b). Within the hinge zone the vein is parasitically folded in conformity with the enclosing sediments. Lineations on parasitic folded surfaces define partial small circles on stereonets (insets, Fig. 3). Near the fold hinge, the gray laminated vein material is characterized by what at first appeared to be a tectonic brecciation, with the influx of milky-white quartz between fragments of the original vein. On closer examination it became apparent that the foliation defined by mica rich surfaces, which is visible to the naked eye, was undisturbed by the fragmentation, and could be aligned either side of the patches of milky quartz (Fig. 4e). Instead of being a brittle dilational feature this 'pseudo-breccia' texture reveals the impact of recrystallization on the laminated vein material without the involvement of any significant displacements or addition of new material.

The geometry of the bedding parallel veins at White Hill, Campbells Creek is less complex (Fig. 3b). A narrow bedding parallel vein is continuous around two adjacent fold hinges with half wavelengths of 17 m. The vein is composed of 5 mm of laminated quartz within shale interbedded with fine- and medium-grained sandstone. In the synclinal hinge the vein is parasitically folded whereas in the intervening limbs the vein is perfectly planar. A strong axial plane pressure solution cleavage has displaced and slightly rotated small segments of the vein near the anticlinal hinge. The vein is slightly thicker on the east limb of the anticline. Here, each layer of laminated quartz has a slightly different lineation direction which gives the vein a fanned appear-

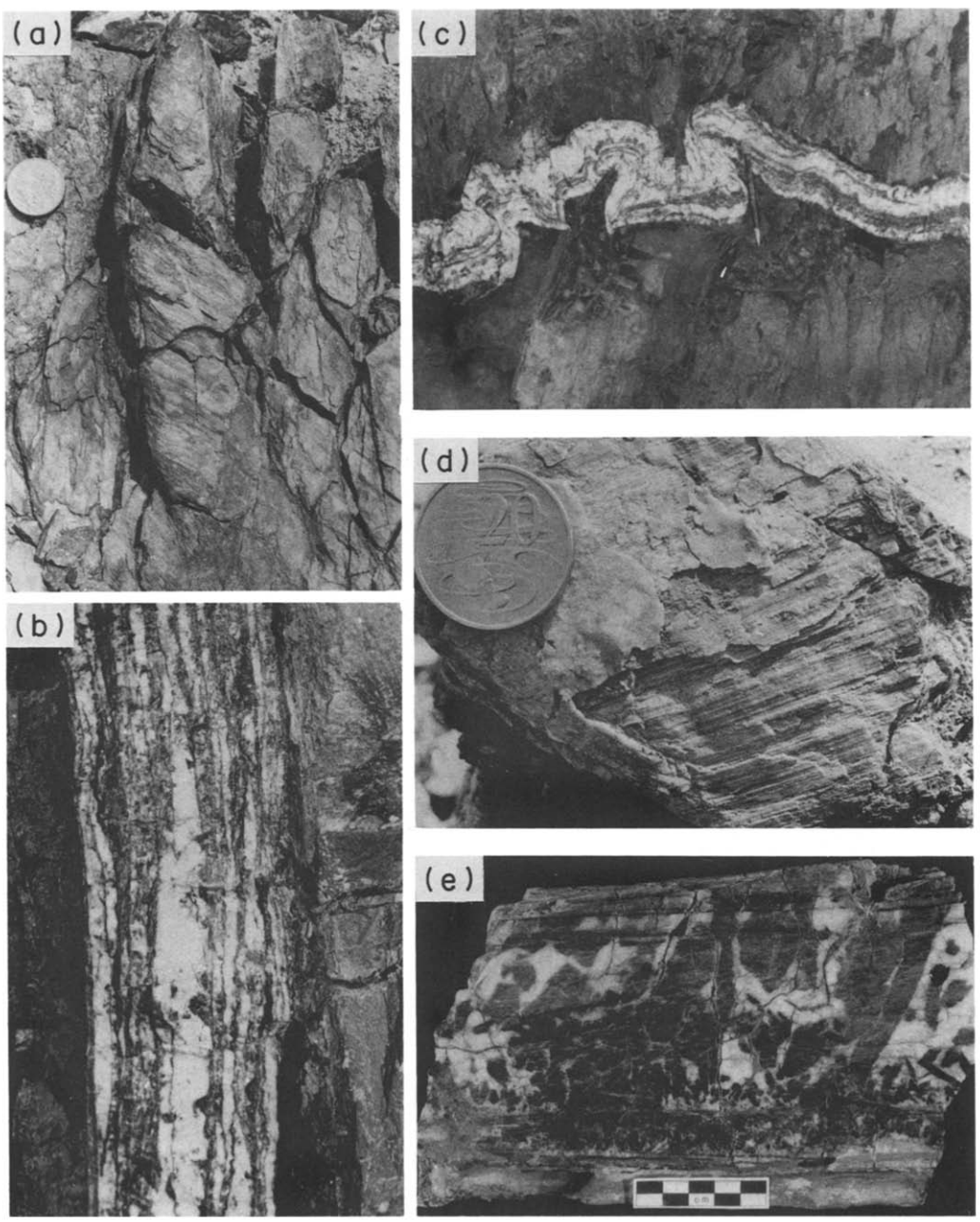

Fig. 4. Field photographs of the bedding parallel veins. (a) Buckled bedding parallel vein (Type I) showing folded quartz elongation lineation. Little Bendigo, Castlemaine (see Fig. 3a). (b) Laminated bedding parallel vein (Type II) showing stylolitic partings and wall rock inclusion bands defining the vein lamination, Central Deborah Mine, Bendigo (see Fig. 2c). Buckled bedding parallel vein (Type II) within the hinge of the Deborah anticline, No. 2 level, Hustler's Reef, Wattle Gully mine, Chewton (see Fig. 2c). (d) Lineated upper surface of bedding parallel vein (Type I) showing consistent lineation direction between successive fibre sheets, Little Bendigo, Castlemaine (see Fig. 3a). (e) 'Pseudo-breccia' due to patchy recrystallization in a bedding parallel vein (Type I) from the hinge zone of the third-order fold, Little Bendigo, Castlemaine (Fig. 3a). The continuity of oblique ISTs either side recrystallized zones can be clearly seen.

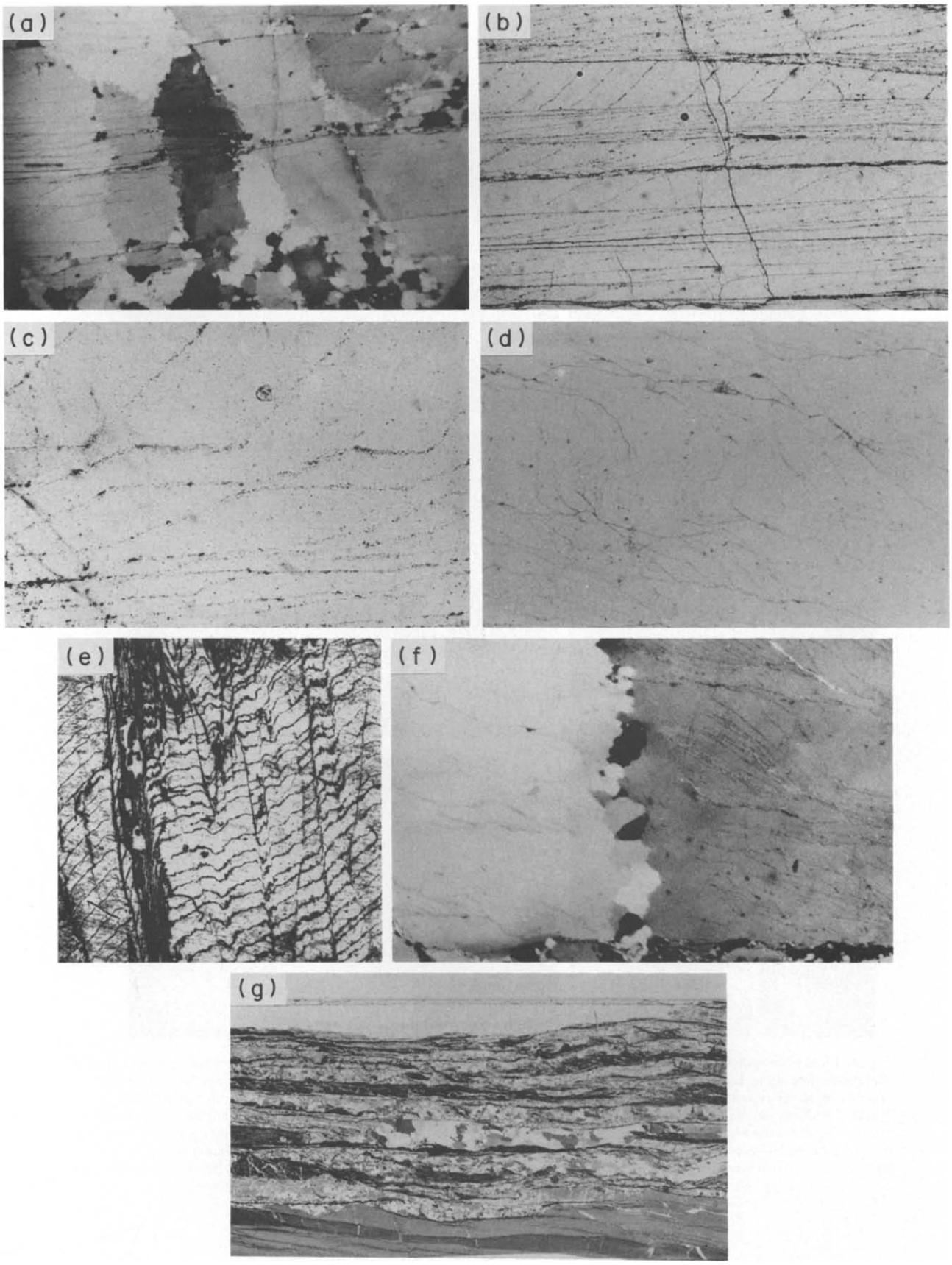
(a)
(b)
(c)
(d)
(e)
(f)
(g)

ance when broken obliquely across the laminations. The quartz lineation direction is constant within individual laminae. Elsewhere along the vein, the lineation is generally sub-perpendicular to the host fold axis.

In the Central Deborah Tourist Mine at Bendigo the No. 5 reef has been exposed by recent development at the No. 2 level. The reef zone is comprised of four narrow bedding parallel veins which occur within a stratigraphic interval of about 5 m (Fig. 2c). Three of the veins are visibly continuous over the hinge of the Deborah anticline and are parasitically folded (Fig. 4). The veins are all truncated by a dyke.

Detailed investigation of mine plans and records (see Appendix 2) has shown that greater than 75% of bedding parallel veins occur at the margin of 'competent' sandstone beds. The mean sandstone layer thickness in these turbidite sequences is approximately 1.7 m (see Appendix 2). The bedding parallel vein spacings are relatively constant (4–15 m) with a mean spacing of 13.2 m (Fig. 7a). Larger vein spacings (> 25 m) tend to be associated with relatively pelite rich parts of the sequence (Fig. 7b); the average pelite content for this section is 44%. Numbers of competent beds between bedding parallel veins range from one to 12 for vein spacings between 3 and 20 m (Fig. 7c).

MICROSTRUCTURE OF BEDDING PARALLEL VEINS

Bedding parallel veins are characterized by laminated quartz from 5 to 300 mm thick which exhibits a down-dip lineation approximately perpendicular to fold axes. Two varieties of laminated quartz can be distinguished in both hand specimen and thin section. These are termed Type I and Type II laminated quartz. The primary microstructures in the two vein types are different in both thin section and hand specimen, and confirm quite distinct histories.

Type I veins

In thin section these veins reveal a complex but regular microstructure. The veins are predominantly quartz, with up to 5% calcite and volumetrically minor amounts of white mica and opaques. The quartz grains are generally elongate, but definitely non-fibrous (Fig. 5a) and their long axes are at a high angle (50–90°) to the vein walls, with a consistent asymmetry. The grains are typically 0.1 mm wide and 0.5 mm long, and do not extend across the width of the vein, but rather interfinger in an irregular manner. In some parts of the vein the quartz is much more equant, and finer grained. The host rock contact with the vein is a 5–10 cm zone of penetratively sheared material showing slickensides on all surfaces parallel to bedding. This slickenside lineation varies in orientation from one surface to another and can make an angle of up to 60° with the vein lineation.

The most striking feature of the Type I veins are the planar arrays of minute included secondary minerals which, in sections cut parallel to the macroscopic lineation and perpendicular to the macroscopic foliation, define a series of inclusion surface traces (ISTs). These show a repeated 'ramp-flat' geometry which is relatively constant parallel to the lineation, but which shows different trace angles progressing from one vein wall to the other (Fig. 8b). The angle between the ISTs and the wall rock varies from 0° to 55°, with a mode of 5–10° and an average of 20° (Fig. 8c). The sense of obliquity of the traces with respect to the wall rock is opposite to that shown by the elongate quartz grains. The inclusions consist predominantly of 5–10 μm white mica grains, which are oriented with their basal planes sub-parallel to the vein walls, and minor opaques.

The ISTs are very regularly spaced in the lineation direction, and form a series of low to high angle oblique features truncated by very low angle (0–5°) traces. The orientation of these surfaces is invariant across quartz grain boundaries; however the ISTs often disappear altogether when they coincide with an area of equant finer grained quartz. The orientation of the parallel sets of high angle traces sometimes varies smoothly between the two confining low angle traces, and the low angle traces themselves can undulate slightly along their length. In some areas (Fig. 5c) the higher angle traces suddenly become vein wall parallel, and then revert to their high angle orientation. This strongly suggests that the continuous low angle traces represent the more general case when the bedding parallel traces coalesce.

In thin sections cut perpendicular to the macroscopic lineation and perpendicular to the macroscopic foliation the ISTs show none of the angular regularity of the sections parallel to the lineation, but instead reveal a

Fig. 5. Photomicrographs of Type I (a–f) and Type II (g) bedding parallel veins. (a) Photomicrograph showing quartz grain morphology, with elongate interfingering grains obliquely oriented with respect to the bedding plane (horizontal). Thin section cut parallel to macroscopic lineation, perpendicular to macroscopic foliation, CN. Field of view is 10 mm across. (b) Geometry of inclusion surface traces (ISTs) showing repeating oscillations between low and high angle sets. Thin section cut parallel to macroscopic lineation, perpendicular to macroscopic foliation, PPL. Field of view is 7 mm across. (c) ISTs showing rapid orientation fluctuations, suggesting that the low angle traces are formed by the coalescence of these low angle steps. Thin section cut parallel to macroscopic lineation, perpendicular to macroscopic foliation, PPL. Field of view is 2 mm across. (d) Anastomosing pattern of ISTs in section cut perpendicular to macroscopic lineation and foliation. Field of view is 7 mm across, PPL. (e) Pattern of ISTs in section cut parallel to macroscopic foliation. Field of view is 5 mm across, PPL. (f) Grain boundary between elongate quartz grains showing that the extent of area swept clean of ISTs extends much further than the present distribution of recrystallized new grains, indicating that the host grains have swept back over the area of new dynamically recrystallized grains. Thin section cut parallel to macroscopic lineation and perpendicular to foliation, CN. Field of view is 7 mm across. (g) Photomicrograph of Type II bedding parallel vein showing disrupted nature of vein, with numerous wall rock slices included and deformed within the vein. Thin section cut parallel to macroscopic lineation, perpendicular to macroscopic foliation. Field of view is 20 mm across, CN. CN = crossed nicols, PPL = plane polarized light.

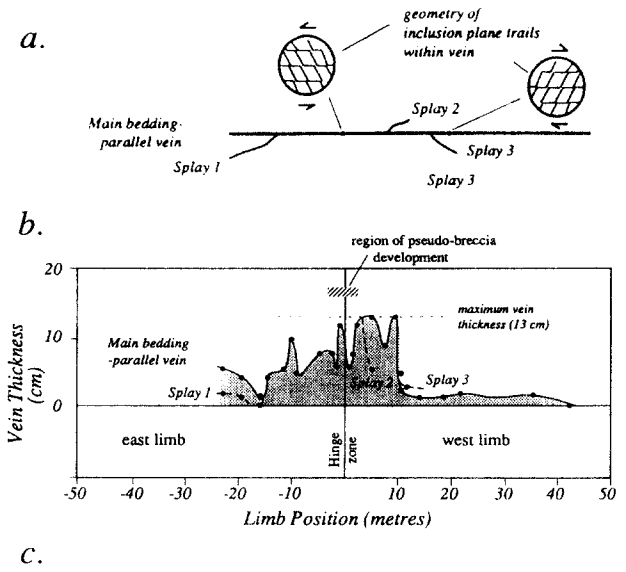

Fig. 6. Vein characteristics of the folded bedding parallel vein at Little Bendigo, Castlemaine (see Fig. 3a). (a) Simplified map of the unfolded vein showing the various splay veins associated with the main bedding parallel vein. (b) Graph of vein thickness (cm) relative to position on the fold recorded as distance (m) from the fold hinge. (c) Vein shape with no thickness exaggeration.

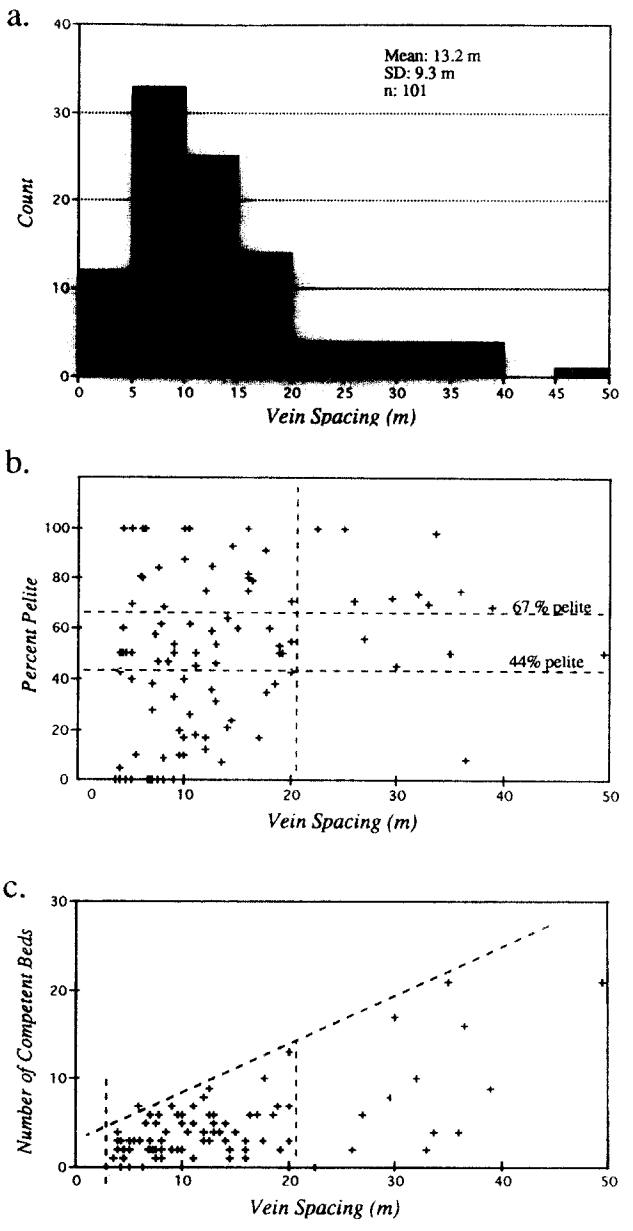

Fig. 7. Statistical data on bedding parallel veins and their association based on investigation of historic detailed 1:360 mine plans (see Table A1). (a) Histogram of vein spacing (m). (b) Graph of vein spacing (m) vs % pelite for individual segments between bedding parallel veins. (c) Graph of vein spacing (m) vs number of competent beds between respective bedding parallel veins.

curved anastomosing pattern (Fig. 5d). In thin sections cut parallel to the macroscopic foliation, the ISTs are either quite straight and sub-parallel to the lineation direction, when the anastomosing low angle planes intersect the surface, or gently curved and sub-perpendicular to the lineation, when the high angle planes intersect the surface (Fig. 5e). The three-dimensional geometry of these planes is thus regular but complex (Fig. 8).

The relationship between the ISTs and the wall rock is generally difficult to decipher, since the vein to bedding-plane interface has acted as a locus for pressure solution and removal of material. However, in thin sections which appear to show unaltered vein–host contacts the boundaries are quite straight in sections cut parallel to the lineation and perpendicular to the foliation. Some stylolites are also visible in the main body of the vein and have the irregular geometries typical of such structures. Also visible in some thin sections are dense arrays of fluid inclusion bands perpendicular to the bedding planes, which cut through both intact and recrystallized grains, and are interpreted as the sites of healed fractures.

Many of the long grain boundaries formed by adjacent elongate quartz grains are marked by fine, equant quartz grains. At these boundaries small offsets or kinks in the ISTs can be seen, suggesting that these small grains were produced during or after small grain boundary shearing episodes. Quartz grains have been found where there has not been any subsequent recrystallization; however in areas where the formation of smaller equant grains is more extensive, the ISTs are removed almost completely. The removal of most of the micas from the ISTs is accompanied by the growth of new, larger micas in the more continuous mica rich surfaces. In some cases the process of new grain formation was followed by a further stage of grain boundary migration. Figure 5(f) shows an original grain boundary containing small equant grains along its length. The area where the ISTs have been removed extends over a much wider area, suggesting that this area at one time was covered by new grains, and that at a later stage these grains were in turn re-consumed by the parent grains. Although these zones bear a superficial resemblance to filled voids produced after cracking (Den Brok & Spiers 1991), the continuity of some ISTs through these zones and the lack of major offsets of ISTs either side of these zones rules out this possibility. This infanticidal behaviour of the parent grains has previously been reported by Means (1989) in the progressive deformation of paradichlorobenzene, so

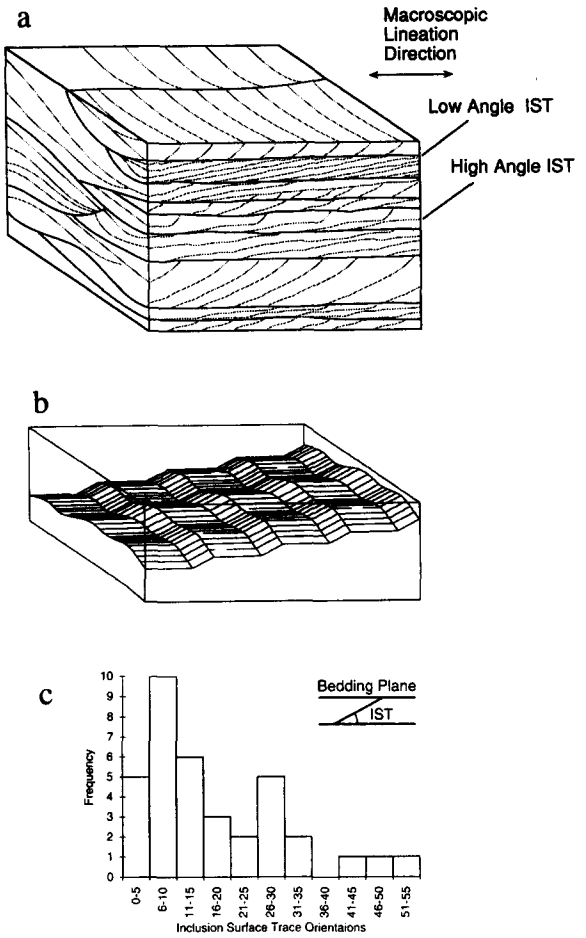

Fig. 8. Schematic diagram showing: (a) three-dimensional geometry of inclusion surfaces in Type I veins; (b) idealized single inclusion surface, showing curved ramp–flat geometry; and (c) frequency distribution of angular separation between local bedding-plane and ISTs.

it is not necessary to invoke two unrelated phases of recrystallization to account for this reversal in fortune of the new grains. These areas of recrystallized quartz with the ISTs swept clean are clear counterparts to the outcrop scale observations of 'pseudo-breccia' near the hinge of the Little Bendigo fold.

Type II veins

Type II veins are much less regular in thin section, and do not show any form of ISTs. Instead there is a high proportion of included and apparently shredded wall rock within the quartz vein material, which itself shows no grain shape preferred orientation (Fig. 5g). The appearance of these veins suggests a more extensive history of movement compared to Type I veins, although we cannot rule out the possibility that they were initially identical and that the present disrupted state represents a second-stage deformation. The quartz is also pervasively disrupted by a complex network of pressure solution seams. The banded nature of these veins has been referred to as 'ribbon structure' and 'book structure' by early workers (e.g. Chace 1949, McKinstry & Ohle 1949).

DISCUSSION

Bedding parallel veins have generally been considered to have formed pre- or early in folding due to build up of high fluid pressures (i.e. $\lambda > 1$, where λ is the ratio of hydrostatic to the lithostatic pressure). Well documented veins in the Wenlock slates of Wales (Nicholson 1964, 1978, Fitches *et al.* 1986, Cosgrove 1993) have been attributed to pre-folding hydraulic jacking open of the bedding by an overpressured pore-fluid to form early bedding-parallel thrusts (Fitches *et al.* 1987, Cosgrove 1993). Localized hydrofracture by fluid packets along bedding-planes could also initiate and localize folding, with fold amplification by a stick–slip mechanism of incremental bedding-slip due to pulsating fluid pressure fluctuations (Price & Cosgrove 1990, pp. 367–384, Cosgrove 1993). If this is the case then bedding parallel vein morphology and microstructure will vary with position across folds. Stick–slip flexural-slip folding models as proposed by Cosgrove (1993) require tapering of veins towards hinge zones due to decreasing slip towards fold hinges. Furthermore, veins along alternate limbs should show opposite displacement sense reflected by vein microstructure either as stepped syntectonic crystal fibres in shear veins (see Ramsay & Huber 1983, pp. 257–261), or as oblique inclusion trials (see van der Pluijm 1984, Cox 1987).

Uniform vein thicknesses across chevron fold hinge zones, as observed in this paper, indicate that veins either formed prior to folding or that significant hinge migration has taken place such that points where veins taper to insignificance represent former hinge positions. The vein microstructure should provide data to reveal the folding mechanisms.

Kinematic models of vein microstructure development

A number of kinematic models have been proposed to explain the microstructural development of bedding parallel veins (see Fig. 9). These include pressure solution, micro-shearing, variable wall rock geometry (Ramsay & Huber 1983, Gaviglio 1986, Labaume *et al.* 1991) and syntaxial vein overgrowth (Cox 1987, this paper). The geometry of the inclusion surface traces and features of the vein microstructures described previously in the paper are used here to assess the suitability of these models of bedding parallel vein development.

Model 1. *Pressure solution seams.* In this model the observed ramp–flat geometry is a result of a two-stage process; in the first stage, a continuous set of high angle ISTs is developed. For this model it is not important quite how they developed, since the final geometry is a result of removal of material by pressure solution in sheets parallel to the bedding plane. Each low angle IST then represents the site of one such pressure solution seam (Fig. 9a). According to this model the angle of the ISTs is a function of the amount of material which has been removed. At first sight this model seems quite promising, since there is evidence for diffusive mass

transfer processes within these veins in the form of stylolites. The geometry of these stylolites is however quite irregular, and is marked by continuous planes of residual minerals. Furthermore, the quartz grain boundaries are truncated by these stylolites. In contrast the boundaries of the low angle ISTs are at most gently curved, and the unrecrystallized quartz grain boundaries are unaffected by these zones.

Model 2. *Micro-shear zones*. As in the previous model, the initial geometry is assumed to be a continuous set of high angle ISTs (Fig. 9b). Once the vein has formed, a series of low angle micro-shear zones offset the ISTs parallel to the bedding planes to form the low angle ISTs. According to this model the angle of the ISTs is a function of the finite shear strain accumulated in a given layer. This model is rejected on the basis of quartz vein microstructure, since in areas where there is evidence of deformation of the vein material, it is accompanied by pervasive recrystallization of the quartz (Fig. 5f). In any case this model would require that the quartz grains themselves were offset, rather than just the ISTs.

Model 3. *Wall rock inclusions*. This model was first proposed by Ramsay & Huber (1983) and has been adopted and modified by Gaviglio (1986) and Labaume *et al.* (1991). In the Ramsay & Huber model, the ISTs represent wall rock inclusions, so that each IST mimics the geometry of the wall rock from which it was spawned, each IST marks a time increment (Fig. 9c), and the translation vector is constrained to be subparallel to the low angle trails seen in Fig. 5(c). In the veins described by these workers, the high angle ISTs were found to be parallel to the walls of en échelon fracture sets, and the low angle ISTs reflect the geometry of throughgoing fractures that link up the en échelon extension fissures. Particularly in the case of the microstructures shown by Labaume *et al.* and Gaviglio, there is good supporting evidence for this model, in the form of clear wall rock fragments that alter the geometry of the adjacent surface, so each surface reflects the change in wall rock geometry. Those wall rock fragments which are found in the Little Bendigo Type I veins are parallel to the bedding planes and appear to be unrelated to the ISTs.

The geometry of the ISTs described here is in general quite distinct from those described by Labaume *et al.* and Gaviglio, in that these ISTs often form at significantly lower angles with respect to the wall rock, often as low as 1–5°, and do not generally display wall rock fragments. Furthermore, in the Little Bendigo veins the wall rock is by definition a bedding plane, and thus does not fit the model of an en échelon fracture surface. If these ISTs did indeed mimic the wall rock geometry we would need a model to explain how straight 1–5° surfaces could develop near bedding plane orientations. The curvature of the ISTs in sections cut parallel to bedding or cut perpendicular to the lineation are also difficult to explain, as these fractures would then have to show strong corrugations in one direction while being quite straight in a perpendicular direction. One further problem with this model is that the translation vector is bedding parallel, so there is no method of actually creating a space for the vein to form in. In summary, this model cannot explain the complex but regular geometry of the ISTs we observe.

Model 4. *Syntaxial wall rock overgrowths*. This model was proposed by Cox (1987) to account for 'inclusion trails' in some quartz veins from the Wattle Gully gold mine, Chewton, an area geographically close to the veins described here. These features are here referred to as *inclusion surface traces* to emphasize their three-dimensional nature. In this model, the ISTs develop as syntaxial overgrowths on a pre-existing cleavage, with each trail tracking the displacement path of the wall rock (Fig. 9d). Thus each set of ISTs was formed synchron-

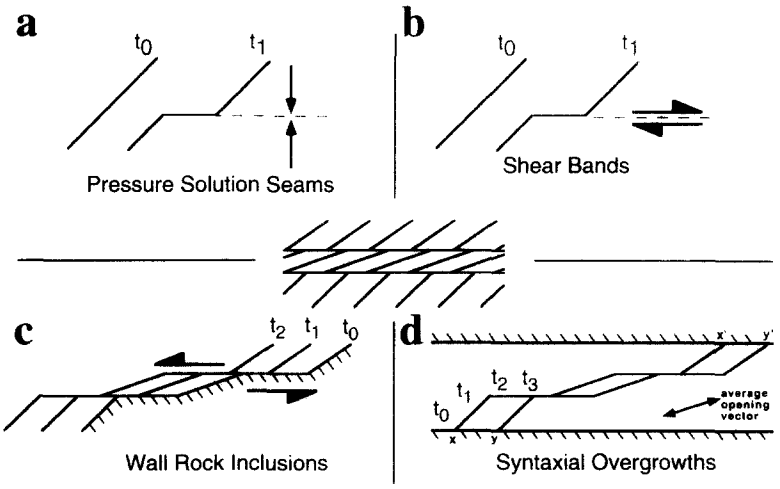

Fig. 9. Models for ramp–flat inclusion surface geometries in Type I veins. (a) Pressure solution seams. (b) Micro shear bands. (c) Wall rock inclusion model proposed by Ramsay & Huber (1983), which assumes that the surfaces represent wall rock fragments removed from ends of dilatant jogs. (d) Syntaxial overgrowths model proposed by Cox (1987), which assumes that the variation in inclusion plane geometry reflects changes in the opening vector; positions x and y were adjacent to positions x′ and y′ prior to vein opening.

ously, with differently oriented sections reflecting different rates of dilation vs translation, so that higher angles reflect relatively faster dilation, and visa versa. In this model the only prerequisites for the nature of the wall rock are that there be some sort of micaceous cleavage and that the surface be somewhat irregular, in order to account for the geometry in sections cut perpendicular to the lineation. The curvature of the ISTs in sections cut perpendicular to the lineation also suggest that the veins opened with a small component of translation in this plane. Examples of extreme curvature of ISTs in this plane (Fig. 5d) are very hard to explain with a wall rock inclusion model; however they are easy to explain if they reflect opening trajectories. The average low angle of the ISTs in sections cut perpendicular to the foliation and parallel to the lineation suggests that vein opening was accompanied by large translational movements. We attempted to verify this model by looking for growth banding using cathodoluminescence, unfortunately the only variations in luminescence correlated with crystallographic orientation. This model is the only one which can easily explain the independent behaviour of the orientations of the quartz grain boundaries and the ISTs, since if the quartz growth is antitaxial it need not be affected by the amount of translation during opening.

The individual micas within each IST are sub-parallel to the bedding planes, and this remains a problem for both this model and the wall rock inclusion model, since presumably the orientation of the micas in a spawning cleavage will be roughly perpendicular to the shortening direction. It is possible that the early stages of inter-layer slip rotated the micas at the bedding surface, as was found in experimentally deformed intact pyrophyllitic clay (Will & Wilson 1989).

In summary the detailed microstructures related to the ISTs suggest that, as with similar microstructures from the same region (Cox 1987), they are indeed tracking the opening vector during vein formation.

Model for bedding parallel vein development in the Bendigo–Castlemaine goldfields

The cycling between low and high angle ISTs is most likely due to some form of fluid pressure–mechanical coupling as has been proposed for faults by Sibson (1985), Sibson *et al.* (1988) and folds by Price & Cosgrove (1990) and Cosgrove (1993). In an environment of externally controlled fluctuating fluid pressures, the bedding-planes will be slightly jacked apart, leading to fold nucleation. Bedding-planes kept apart by high fluid pressures should allow faster slip along the bedding-planes, without greatly modifying the dilation rate, which in turn will lead to higher translation to dilation ratios, and lower angle ISTs.

As such, the ISTs should reveal the kinematic history of the vein development and the folds that host them. The overall two-dimensional vein geometry is that of a doubly tapering wedge centred on the fold hinge, which

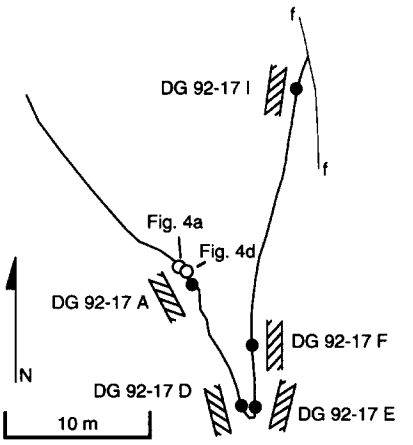

Fig. 10. Map showing the geometry of the inclusion plane traces in the Type I veins at different locations from the Little Bendigo fold (Fig. 3a), together with outcrop photograph localities. The relationship between inclusion surface trace and bedding is schematically displayed at each locality and shows that the asymmetry is mirrored across the fold axial plane. Based on thin sections DG 92-17 A,D,E,F and I.

implies that the vein and the fold are genetically related in some way; the geometry of the ISTs at the Little Bendigo fold has been mapped out and is shown schematically in Fig. 10. The obliquity of the ISTs switches across the fold hinge, again implying a genetic relationship. The same asymmetry of the ISTs with respect to the fold hinge has also be seen in a vein from the one exposed limb of the Garden Gully Anticline (Fig. 1).

These veins cannot be directly related to the main amplification phase of the folding as vein lineations are clearly folded around second-order folds. Furthermore, extensive recrystallization, leading to the formation of the 'pseudo-breccia', is concentrated in the hinges of the folds suggesting that hinge tightening post-dates the formation of the veins. Finally, the shear sense inferred from the ISTs is opposite in sense to that which would be expected from a flexural-slip fold.

The veins must have formed in the earliest stages of fold development and are considered to be a crucial part of the fold nucleation process. A model is proposed where an essentially undeformed multilayer compressed parallel to the layering undergoes a period of layer parallel shortening prior to the fold amplification stage (e.g. Dietrich 1970, Stephansson & Berner 1971). The amount of shortening prior to buckling and the rate of amplification of single layers has been shown to vary according to layer thickness and competency contrast with the host rock (Hudleston & Stephansson 1973). In multilayers the possibility of adjacent layers undergoing distinct layer parallel shortening and early amplification histories is increased when cohesion between the layers is weak or non-existent. In this low cohesion case one layer can potentially start to buckle while an adjacent layer is still shortening, which would produce a planar void, and the displacement vectors across the void would be opposite in sense to those predicted by a flexural-slip model (Fig. 11).

As the buckling layer reaches a significant limb dip, it

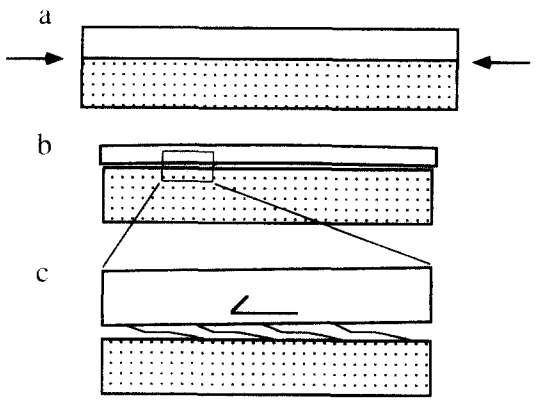

Fig. 11. Cartoon of vein formation during the earliest stages of fold nucleation. (a) Two layers from a larger multilayer system, distinguished in this case by thickness, but possibly also by stiffness and lateral variations in these two properties. (b) As a result of undergoing distinct layer parallel shortening histories, the top layer starts to buckle first, producing a narrow opening. (c) In detail the veins that fill this opening will show a sense of displacement opposite to that which develops during flexural-slip folding.

is likely that the adjacent layer will also start to buckle. In order to explain the Little Bendigo fold, with a void 15 cm thick and 100 m long (50 m each side of the 'hinge'), we only need a limb dip of 0.17°. Assuming that during the early stage of differential layer parallel shortening one layer shortened from 100 m by 10% and the other by 12.5%, this would result in a relative length mismatch of 2.5 m and give an average opening vector of about 7° away from the plane of the bedding. In order to test this model more carefully the relative displacements of the layers at various locations along the vein would need to be known; however, a lack of markers in the host rocks and the difficulty in following individual ISTs through low angle zones has prevented this.

Once the vein and proto-fold has developed it would of course be an ideal locus for any future buckling and fold amplification by conventional flexural-slip mechanics. As stated earlier, the best candidate for the linear features on the bedding planes which spawned the ISTs was a bedding–cleavage intersection lineation, requiring cleavage formation very early in the compression history. The regularity of spacing of adjacent inclusion trails may reflect the spacing of a pre-existing cleavage at the time of formation of the veins. The orientation of the cleavage is consistent with the compression direction assumed to have formed the major folds; however, it certainly does not reflect the present-day cleavage spacing.

The flexural-slip folding is itself associated with slip on the bedding planes. However, this slip is concentrated on the limbs of the fold thus preserving the microstructures in the Type I veins, except actually at the hinge, where the small radius of curvature of the bending has induced recrystallization of the vein to produce the 'pseudo-breccia' texture. The main amplification of the fold could also have produced the sheared and slickensided margins to the veins. Much larger inter-bed slips associated with flexural slip folding have resulted in the formation of the highly disrupted Type II veins, where there is no lateral continuity of microstructure.

CONCLUSIONS

The field and microstructural data from the Bendigo–Castlemaine region (Lachlan Fold Belt, Australia) suggest a model for multilayer fold nucleation that may be applicable to other regions. The veins we have studied have the following characteristics.

(1) Bedding parallel veins have distinct character and morphology relative to other tectonic veins. They have high length to thickness ratios, remarkable lateral continuity (e.g. 85 m across strike and 3.2 km along strike maximum recorded lengths, Bendigo goldfield), relatively uniform thickness (commonly <20 cm) and are most common in turbidite sequences (see also Fitches *et al.* 1986, Mawer 1987, Tanner 1989).

(2) Bedding parallel veins in the Bendigo goldfield are more common at the margins of sandstone beds and have a relatively consistent spacing of 13 m in interbedded sandstone and mudstone sequences with approximately equal proportions of sandstone and mudstone and where mean sandstone bed thickness is 1.7 m. When mudstone predominates the bedding parallel vein spacing is less regular and may be as high as 40 m.

(3) The veins are intimately associated with and folded by chevron folds. Quartz fibre elongation lineations in the veins are commonly at high angles to observed mesoscopic fold hinges.

(4) These veins have two morphological forms. Type I veins are thin (5–10 cm) laminated veins consisting of stacked, millimetre thick subparallel sheets of quartz with complex microstructure dominated by phyllosilicate inclusion surfaces. Type II veins are thicker (generally <20 cm), banded veins composed of alternating milky-white quartz and wall rock bounded by stylolitic partings parallel to the margins of the veins.

(5) The small-scale folding and recrystallization of the Type I bedding parallel veins suggests that they formed prior to the main amplification phase of the folding, but their location at fold hinges indicate that they are not totally unrelated.

(6) Inclusion surface traces (ISTs) seen in the Type I veins from this region are inconsistent with an origin related to wall rock geometry, and instead seem to reflect the opening history of the veins. The microstructures in the Type I veins, together with their field relations with respect to the present day folds, suggest that they track the incremental opening vector and formed during early fold nucleation, possibly associated with the differences in layer parallel shortening relative to buckling for individual layers in a sedimentary pile.

(7) The cycling between high and low angle ISTs could be related to cycling of fluid pressures during vein formation. Fluid pressure fluctuations probably controlled the relative rates of translation vs dilation during hydraulic jacking of bedding partings to form the veins.

(8) The disrupted layering and inclusion of wall rock

slivers suggest that Type II veins formed during the main amplification stage of the folds.

Acknowledgements—The research was supported by Australian Research Council grants ARC E831566 (Gray) and ARC A38615754 (Durney, Gray and Gregory). The research on bedding parallel veins was initiated as part of an M.Sc degree by C. E. Willman at Monash University. We would like to thank Janos Urai, Stephen F. Cox, Geoff Tanner and Sue Treagus for their thoughtful and detailed comments during review.

REFERENCES

Behzadi, H. & Dubey, A. K. 1980. Variation of interlayer slip in space and time during flexural folding. *J. Struct. Geol.* **2**, 453–457.

Caldwell, J. J. 1942. North Deborah, Bendigo. *Min. Geol. J. Vict. Dept. Mines* **2**, 318–319.

Chace, F. M. 1949. Origin of the Bendigo saddle reefs with comments on the formation of ribbon quartz. *Econ. Geol.* **44**, 561–597.

Cosgrove, J. W. 1993. The interplay between fluids, folds and thrusts during the deformation of a sedimentary succession. *J. Struct. Geol.* **15**, 491–500.

Cox, S. F. 1987. Antitaxial crack-seal vein microstructures and their relationship to displacement paths. *J. Struct. Geol.* **9**, 779–787.

Cox, S. F. & Etheridge, M. A. 1983. Crack-seal fibre growth mechanisms and their significance in the development of oriented layer silicate microstructures. *Tectonophysics* **92**, 147–170.

Cox, S. F., Etheridge, M. A., Cas, R. A. F. & Clifford, B. A. 1991a. Deformational style of the Castlemaine area, Bendigo–Ballarat zone: Implications for evolution of crustal structure in central Victoria. *Aust. J. Earth Sci.* **38**, 151–170.

Cox, S. F., Wall, V. J., Etheridge, M. A. & Potter, T. F. 1991b. Deformational and metamorphic processes in the formation of mesothermal vein-hosted gold deposits—examples from the Lachlan Fold belt in central Victoria, Australia. *Ore Geol. Rev.* **6**, 391–423.

Den Brok, S. W. J. & Spiers, C. J. 1991. Experimental evidence for water weakening of quartzite by microcracking plus solution-precipitation creep. *J. geol. Soc. Lond.* **148**, 541–548.

de Sitter, L. U. 1964. *Structural Geology* (2nd edn). McGraw-Hill, New York.

Dietrich, J. H. 1970. Computer experiments on mechanics of finite amplitude folds. *Can. J. Earth Sci.* **7**, 467–476.

Dunn, E. J. 1896. Reports on the Bendigo goldfield. Special Reports, Victoria Mines Department.

Fitches, W. R., Cave, R., Craig, J. & Maltman, A. J. 1986. Early veins as evidence of detachment in the Lower Palaeozoic rocks of the Welsh Basin. *J. Struct. Geol.* **8**, 607–620.

Gaviglio, P. 1986. Crack-seal mechanism in a limestone: a factor of deformation in strike-slip faulting. *Tectonophysics* **131**, 247–255.

Ghosh, S. K. 1968. Experiments of buckling of multilayers which permit interlayer gliding. *Tectonophysics* **6**, 207–249.

Gray, D. R. 1988. Structure and tectonics of Victoria. In: *Geology of Victoria* (edited by Douglas, J. G. & Ferguson, J. A.). 1–36.

Gray, D. R., Gregory, R. T. & Durney, D. W. 1991b. Rock-buffered fluid–rock interaction in deformed quartz-rich turbidite sequences, eastern Australia. *J. geophys. Res.* **96**, 19681–19704.

Gray, D. R. & Willman, C. E. 1991a. Deformation in the Ballarat Slate belt, central Victoria and implications for the crustal structure across southeastern Australia. *Aust. J. Earth Sci.* **38**, 171–201.

Gray, D. R. & Willman, C. E. 1991b. Thrust-related strain gradients and thrusting mechanisms in a chevron-folded sequence, southeastern Australia. *J. Struct. Geol.* **13**, 691–710.

Gray, D. R., Wilson, C. J. L. & Barton, T. J. 1991a. Intracrustal detachments and implications for crustal evolution within the Lachlan Fold Belt, southeastern Australia. *Geology* **19**, 574–577.

Henderson, J. R., Henderson, N. M. & Wright, T. O. 1990. Water-sill hypothesis for the origin of certain veins in the Meguma Group, Nova Scotia, Canada. *Geology* **18**, 654–657.

Hudleston, P. J. 1973. An analysis of 'single layer' folds developed in a viscous media. *Tectonophysics* **16**, 189–214.

Hudleston, P. J. & Stephansson, O. 1973. Layer shortening and fold-shape development in the buckling of single layers. *Tectonophysics* **17**, 299–321.

Labaume, P., Berty, C. & Laurent, Ph. 1991. Syn-diagenetic evolution of shear structures in superficial nappes: an example from the Northern Apennines (NW Italy). *J. Struct. Geol.* **13**, 385–398.

McKinstry, H. E. & Ohle, E. L. 1949. Ribbon structure in gold–quartz veins. *Econ. Geol.* **44**, 87–109.

Mawer, C. K. 1987. The formation of gold-bearing quartz veins, Nova Scotia, Canada. *Tectonophysics* **135**, 99–119.

Means, W. D. 1989. Synkinematic microscopy of transparent polycrystals. *J. Struct. Geol.* **11**, 163–174.

Nicholson, R. 1964. Fabric analysis of a deformed vein. *Geol. Mag.* **101**, 474.

Nicholson, R. 1978. Folding and pressure solution in a laminated quartz–calcite vein from the Silurian slates of the Llangollen region of North Wales. *Geol. Mag.* **115**, 47–54.

Odling, N. 1987. The determination of 'buckling rotation' and its application to theoretical and experimental models of buckle folds. *J. Struct. Geol.* **9**, 1021–1028.

Price, N. J. & Cosgrove, J. W. 1990. *The Analysis of Geological Structures*. Cambridge University Press, Cambridge.

Ramsay, J. G. 1967. *Folding and Fracturing of Rocks*. McGraw-Hill, New York.

Ramsay, J. G. 1974. Development of chevron folds. *Bull geol. Soc. Am.* **85**, 1741–1754.

Ramsay, J. G. 1980. The crack-seal mechanism of rock deformation. *Nature, Lond.* **284**, 135–139.

Ramsay, J. G. & Huber, M. I. 1983. *The Techniques of Modern Structural Geology, Volume* 1: *Strain Analysis*. Academic Press, London.

Roering, C. & Smit, C. A. 1987. Bedding-parallel shear, thrusting and quartz vein formation in Witwatersrand quartzites. *J. Struct. Geol.* **9**, 419–427.

Sibson, R. H. 1985. A note on fault reactivation. *J. Struct. Geol.* **7**, 751–754.

Sibson, R. H., Roberts, F. & Poulson, K. M. 1988. High angle reverse faults, fluid pressure cycling and mesothermal gold deposits. *Geology* **16**, 551–555.

Stephansson, O. & Berner, H. 1971. The finite element method in tectonic processes. *Phys. Earth & Planet. Interiors* **4**, 301–321.

Stephens, M. B., Glassons, M. J. & Keays, R. R. 1979. Structural and chemical aspects of metamorphic layering development in metasediments from Clunes, Australia. *Am. J. Sci.* **279**, 129–160.

Stillwell, F. L. 1917. The factors influencing gold deposition in the Bendigo Goldfield. *Bull. Comm. Aust. Adv. Coun. Sci. & Ind.* **4**.

Tanner, F. W. G. 1989. The flexural-slip mechanism. *J. Struct. Geol.* **11**, 635–655.

Tanner, F. W. G. 1990. The flexural-slip mechanism: Reply. *J. Struct. Geol.* **12**, 1084–1087.

Thomas, D. E. 1953. Mineralisation and its relationship to the geological structure of Victoria. In: *Geology of Australian Ore Deposits* (edited by Edwards, A. B.). Australasian Institute Mining and Metallurgy, Melbourne, 971–985.

van der Pluijm, B. A. 1984. An unusual "crack-seal" vein geometry. *J. Struct. Geol.* **6**, 593–597.

Waldron, H. M. & Sandiford, M. 1989. Deformation volume and cleavage development in metasedimentary rocks from the Ballarat Slate Belt. *J. Struct. Geol.* **10**, 53–62.

Whitelaw, H. S. 1914. Hustler's line of reef, Bendigo. *Geol. Surv. Vic. Bull.* **33**.

Whitelaw, H. S. 1918. The Confidence group of mines. *Geol. Surv. Vic. Bull.* **41**.

Will, T. M. & Wilson, C. J. L. 1989. Experimentally produced slickenside lineations in pyrophylitic clay. *J. Struct. Geol.* **11**, 657–668.

Willman, C. E. 1988. Geological Report: Spring Gully 1:10,000 map area, Bendigo goldfield. *Vic. geol. Surv. Rep.* **85**.

Willman, C. E. & Wilkinson, H. E. 1992. Geological Report: Bendigo Goldfield (Spring Gully, Golden Square, Eaglehawk 1:10,000 maps). *Vic. geol. Surv. Rep.* **93**.

APPENDIX

Table A1. Locations of bedding parallel veins studied in this paper

Station	Location	Vein Type
DG84-129	Pioneer Mine, One Tree Hill, Bendigo (AMG 259720E/5923470N)	Type II
DG84-132	Burns Street road cutting, south Bendigo (AMG 257350E/5934000N)	Type I
DG84-133	Diamond Hill, road cutting near intersection with Burns road, South Bendigo (AMG: 256220E/5923390N)	Type I
DG92-17	bedrock outcrop beside road, Little Bendigo (AMG: 254140E/5892620N)	Type I
DG88-64	Central Deborah Mine, Level 2, Bendigo (AMG: 256590E/5926500N)	Type II
CW83-13	White Hills, Campbells Creek (AMG: 251970E/5890800N)	Type II

Table A2. Bedding parallel vein data from 1:360 scale mine plans of the Bendigo goldfield

Mine name	Vein	Vein width	Max C.B.T.	No. C.B.	Mean C.B.T.	Vein spacing	% pelite	Total pelite	Total psammite
Virginia	1	12.0	3.0	6		18.5	38	7.03	11.47
	2		2.5	5	1.80	11.0	18	1.98	9.02
	3	100.0	2.0	2	1.00	7.2	58	4.20	3.00
	4		3.0	5	1.10	10.0	17	1.70	8.30
	5	25.0	2.0	2	1.90	7.0	28	1.96	5.04
	6	12.0	8.0	3	3.50	20.0	43	17.20	2.80
	7	150.0	3.0	4	1.80	10.5	26	2.73	7.77
	8	25.0	1.8	6	1.00	7.0	0	0.00	7.00
	9	12.0	2.2	7	1.20	9.0	0	0.00	9.00
	10		1.0	3	0.67	5.0	40	2.00	3.00
	11	25.0	3.0	3	1.66	5.0	0	0.00	5.00
	12	5.0	5.5	3		8.0	0	0.00	8.00
Specimen Hill	1	12.0	2.8	10	1.07	32.0	74	23.68	8.32
	2		7.0	1	7.00	8.0	9	0.56	7.44
	3	11.0	7.0	2	7.00	4.0	43	1.72	2.28
	4		6.4	17	1.46	30.0	45	13.50	16.50
	5		0.8	2	0.50	33.0	70	23.10	9.90
	6		1.8	7	0.64	5.9	81	4.80	1.10
	7	50.0	1.2	6	0.50	7.8	62	4.84	2.96
	8		0.8	2	0.60	10.0	88	8.80	1.20
	9	12.0				5.0	100	5.00	0.00
	10	25.0	0.4	13	0.40	20.0	71	14.20	5.80
	12	25.0	0.5	3	0.46	4.2	60	2.52	1.68
	13					10.4	100	10.40	0.00
	14		0.5	3	0.50	17.6	91	16.02	1.58
Nth Argus	1		4.8	2	3.80	26.0	71	18.46	7.54
	2	25.0	2.0	10	1.00	17.7	35	6.19	11.51
	3		2.8	2	2.80	19.2	50	9.60	9.60
	4	6.0	3.1	4	1.10	33.6	98	32.93	0.67
	5	6.0	1.0	1	1.00	14.4	93	13.39	1.01
	6	6.0	4.8	3	3.40	12.5	85	10.62	1.88
	7		3.8	6	1.70	16.3	79	12.88	3.42
	8	12.0	2.1	6	1.30	9.6	20	1.92	7.68
Pearl Mine	1		1.0	4	1.00	10.5	62	6.51	3.99
	2		1.7	2	1.25	5.0	50	2.50	2.50
	3		0.8	7	0.60	9.0	50	4.50	4.50
	4					10.0	100	10.00	0.00
	5		2.0	2	2.00	7.5	47	3.52	3.98
	6		1.0	4	1.00	8.5	47	3.99	4.51
	7		1.2	7	0.50	11.0	45	4.95	6.05
	8	100.0	3.0	4	1.60	13.0	31	4.03	8.97
	9	50.0	1.8	2	1.80	9.0	54	4.86	4.14
	10		5.5	1	5.50	11.0	50	5.50	5.50
Comet Mine	1	gouge	3.0	4	2.00	36.0	75	27.00	9.00
	2	25.0	1.8	3	1.20	16.0	82	13.12	2.88
	3		2.5	3	1.30	4.0	0	0.00	4.00
	4	300.0	1.0	2	1.00	4.0	50	2.00	2.00
	5		3.0	21	1.00	35.0	50	17.50	17.50
	6	25.0	3.1	5	1.50	7.5	0	0.00	7.50
	7	150.0	4.0	6	2.20	17.0	17	2.89	14.11
	8	50.0	3.5	4	1.90	12.0	17	2.04	9.96
	9	75.0	4.2	5	2.40	14.0	21	2.94	11.06

Table A2. *Continued*

Mine name	Vein	Vein width	Max C.B.T.	No. C.B.	Mean C.B.T.	Vein spacing	% pelite	Total pelite	Total psammite
Great Ext.	1	12.5	3.5	2	3.40	6.8	0	0.00	6.80
Hustlers	2		3.0	6	0.90	13.0	54	7.02	5.98
	3		2.1	3	1.50	14.0	64	8.96	5.04
	4	25.0	0.3	numerous	0.30	18.0	60	10.80	7.20
	5		1.8	9	0.80	12.5	36	4.50	8.00
	6	25.0	2.0	7	1.00	19.0	53	10.07	8.93
	7	100.0	8.0	2	5.50	14.5	24	3.48	11.02
	8	25.0	3.2	3	1.50	7.0	38	2.66	4.34
	9	50.0	2.2	8	1.00	12.0	12	1.44	10.56
	10	75.0	2.0	3	1.30	4.0	5	0.20	3.80
	11	5.0	4.1	21	1.00	49.5	50	24.75	24.75
	12	75.0	5.0	6	2.00	27.0	56	15.12	11.88
	13		2.5	7	1.10	19.0	50	9.50	9.50
United Hustlers	1	12.0	4.5	2	4.50	10.0	10	1.00	9.00
& Redan	2	gouge	1.1	6	0.80	10.0	40	4.00	6.00
	3	12.0	7.5	16	1.80	36.5	8	2.92	33.58
	4	25.0	4.0	5	1.20	6.5	0	0.00	6.50
	5	gouge		0		4.2	100	4.20	0.00
	6	25.0	2.6	3	1.10	16.0	80	12.80	3.20
	7	50.0	1.0	3	0.50	4.2	50	2.10	2.10
	8	75.0		0		5.0	100	5.00	0.00
	9	125.0		0		22.5	100	22.50	0.00
	10		1.2	1	1.20	7.5	84	6.30	1.20
	11	50.0	1.6	4	0.70	4.0	5	0.20	3.80
Hustlers Reef	1	150.0	3.0	4	1.60	15.0	60	9.00	6.00
	2	gouge		0		6.2	100	6.20	0.00
	3	6.0	1.0	2	0.75	5.0	70	3.50	1.50
	4	75.0	1.6	5	1.10	13.0	46	5.98	7.02
	5	330.0	2.0	2	1.12	8.0	69	5.52	2.48
	6	75.0	2.5	7	1.18	20.0	55	11.00	9.00
	7	150.0	3.7	2	3.00	9.0	33	2.97	6.03
Hustlers Reef	1	150.0				25.0	100	25.00	0.00
No. 1	2	150.0	4.5	2	3.75	9.5	10	0.95	8.55
	3	25.0				6.0	100	6.00	0.00
	4	150.0	1.0	3	1.00	12.0	75	9.00	3.00
	5		2.0	2	1.25	4.5	50	2.25	2.25
	6	12.0	1.8	6	0.80	12.5	59	7.37	5.13
	7	12.0	1.9	3	1.60	5.5	10	0.55	4.95
	8		0.3	3	0.30	6.0	80	4.80	1.20
	9	50.0	1.0	2	1.00	4.0	50	2.00	2.00
KK Mine	1	200.0	3.0	9	1.10	39.0	69	26.91	12.09
	2	12.0				6.0	100	6.00	0.00
	3	12.0	2.5	2	2.00	16.0	75	12.00	4.00
	4	12.0	4.5	1	4.50	4.5	0	0.00	4.50
	5	75.0	2.0	8	1.00	29.5	72	21.24	8.26
	6	25.0	4.1	4	2.60	13.5	7	0.94	12.56
	7	150.0	1.0	1	1.00	16.0	100	16.00	0.00
	8	100.0	3.5	1	3.50	3.5	0	0.00	3.50
	9	100.0				6.0	100	6.00	0.00
MEANS		61.5	2.7	5	1.69	13.2			
TOTALS						1333.0		742.50	590.80

Mine name: mine from which vein data was obtained (for locations see Fig. 1).
Vein: refers to an arbitrary number given to veins, but vein 1 is stratigraphically higher than vein 2, etc.
Width (mm): width of vein in millimetres. If no quartz is present then there is no entry. If fault gouge is present then the gouge is recorded.
Max C.B.T: refers to the maximum thickness (metres) of all sandstone beds within the interval from vein 1 to vein 2, etc.
No. C.B.: number of sandstone beds.
Mean C.B.T.: mean competent bed thickness (metres).
Spacing: stratigraphic thickness (metres) between successive veins; spacing from vein 1 is taken as the interval from vein 1 to vein 2.
% pelite: (total cumulative pelite/stratigraphic thickness) × 100.
Total pelite: total cumulative thickness (metres) of pelite between vein 1 and vein 2, etc.
Total psammite: total cumulative thickness of psammite (metres) between vein 1 and vein 2, etc.